Falling clouds of particles

Élisabeth Guazzelli

IUSTI – CNRS – Aix-Marseille Université
elisabeth.guazzelli@polytech.univ-mrs.fr

Dispersion of Sphagnum Moss Spores
Whitaker & Edwards Science 2010

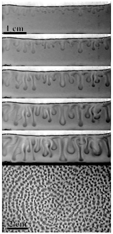

Bioconvection
Jánosi, Kessler & Horváth PRE 1998

"Specifically, we consider the motion under gravity of particles within a blob (a convenient term for a finite volume of a dispersion of particles in liquid) comprising a large number N of particles initially distributed randomly in liquid with uniform mean concentration within a prescribed closed surface, and inquire as to its subsequent time evolution. The particles will tend to spread out from each other, and questions of interest are therefore: do particles leave the blob, and if so how, and what is the lifetime of the blob as a cohesive entity?"

Nitsche and Batchelor JFM 1997

1. A cloud of spheres at low Reynolds number
   - Stability of the cloud
   - Influence of initial shape
   - Particle leakage
   - Breakup
2. And also a cloud of fibers
3. Beyond Stokes flow: A cloud at finite Reynolds number
   - Scalings and dimensionless numbers
   - Regimes of macro-scale and micro-scale inertia
   - Instability and breakup
4. Conclusions

Sedimentation of a single sphere

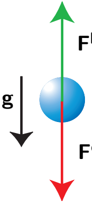

$\mathbf{F^h} = -6\pi\mu a\,\mathbf{U_S}$

$\mathbf{F^e} = \frac{4}{3}\pi a^3(\rho_p - \rho_f)\,\mathbf{g}$

Stokes velocity:

$$\mathbf{U_S} = 2(\rho_p - \rho_f)a^2\mathbf{g}/9\mu$$

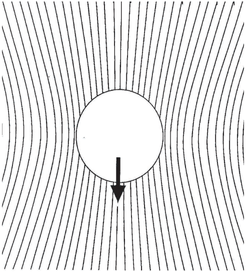

Stokes 1851

$$\mathbf{u} = \left(\frac{\mathbf{I}}{r} + \frac{\mathbf{xx}}{r^3}\right)\cdot\frac{\mathbf{F^e}}{8\pi\mu} + \left(\frac{\mathbf{I}}{3r^3} - \frac{\mathbf{xx}}{r^5}\right)\cdot\frac{a^2\mathbf{F^e}}{8\pi\mu}$$

Long-range interactions: $u \sim O(\frac{aU_S}{r})$

Spherical cloud of spheres

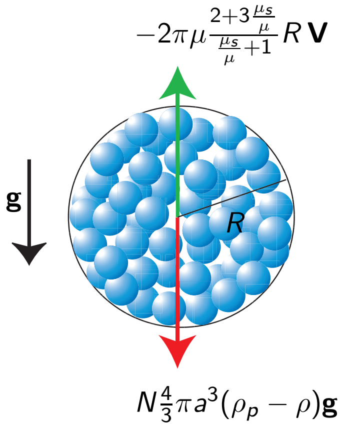

- Drag force (Hadamard, Rybczyński 1911)

$$\mathbf{F^h} = -2\pi\mu\frac{2+3\frac{\mu_s}{\mu}}{\frac{\mu_s}{\mu}+1}R\,\mathbf{V}$$

- Settling velocity

$$\mathbf{V} = \frac{N\frac{4}{3}\pi a^3(\rho_p-\rho)\mathbf{g}}{2\pi\mu\frac{2+3\frac{\mu_s}{\mu}}{\frac{\mu_s}{\mu}+1}R} \approx \frac{N\frac{4}{3}\pi a^3(\rho_p-\rho)\mathbf{g}}{5\pi\mu R}$$

Continuous spherical distribution of excess mass

Flow field inside a falling drop

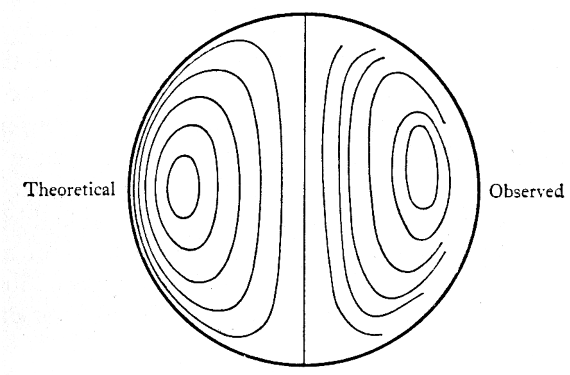

from Batchelor 1970

Toroidal circulation

Stability of the cloud?

- "A spherical blob shape is especially well suited to a study of random particle migration across interface because the gravity-driven flow maintains essentially constant form" (Nitsche & Batchelor JFM 1997).
- "An initially spherical blob does not substantially change its shape when falling" (Machu, Meile, Nitsche & Schaflinger JFM 2000).
- "In the case of low Reynolds numbers, the suspension drop retains a roughly spherical shape while settling" (Bosse, Kleiser, Härtel & Meiburg PoF 2005).

But the cloud is unstable!

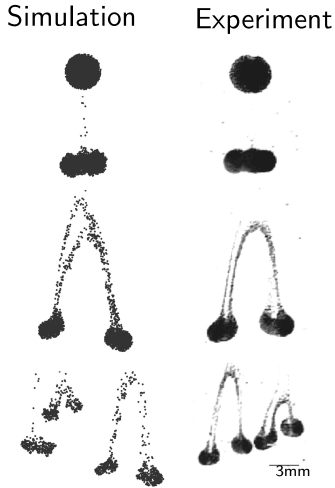

Metzger, Nicolas & Guazzelli JFM 2007

Point-force model: The Stokeslet

- Minimal description: ONLY far-field and strictly $Re = 0$

$$\dot{\mathbf{r}}_i = \mathbf{U_S} + \frac{\mathbf{F^e}}{8\pi\mu} \cdot \sum_{j \neq i} \left(\frac{\mathbf{I}}{|\mathbf{r^*_{ij}}|} + \frac{\mathbf{r_{ij}r_{ij}}}{|\mathbf{r^*_{ij}}|^3} \right)$$

with $\mathbf{r}_{ij} \equiv \mathbf{r}_i - \mathbf{r}_j$

- Dimensionless equations (length-scale $= R_0$ and velocity-scale $= V_0 = \frac{N_0 F}{5\pi\mu R_0}$ of the initially spherical cloud)

$$\dot{\mathbf{r}}^*{}_i = \frac{5R_0}{6N_0 a} \cdot \mathbf{e}_g + \frac{5}{8N_0} \sum_{j \neq i} \left(\frac{\mathbf{I}}{|\mathbf{r^*_{ij}}|} + \frac{\mathbf{r_{ij}r_{ij}}}{|\mathbf{r^*_{ij}}|^3} \right) \cdot \mathbf{e_g}$$

Ekiel-Jeżewska, Metzger & Guazzelli PoF 2006
Metzger, Nicolas & Guazzelli JFM 2007

Evolution of the cloud

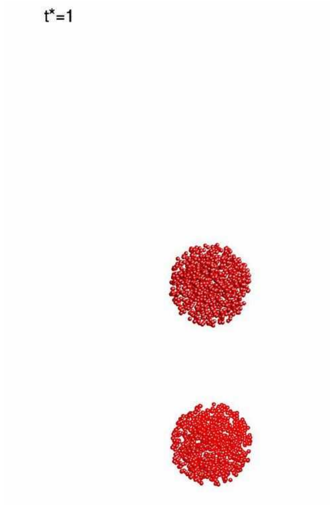

Break-up probability and time

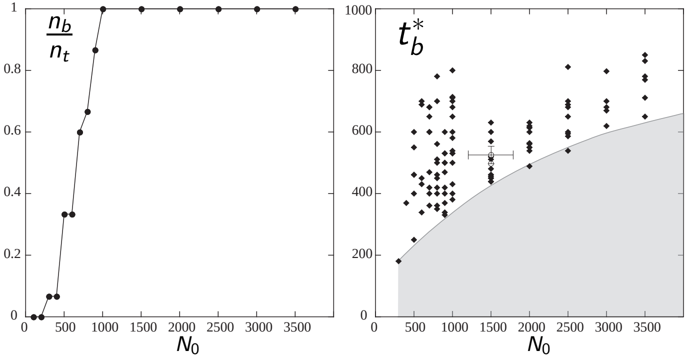

Sole dependance on N_0

Successive numerical-cloud profiles

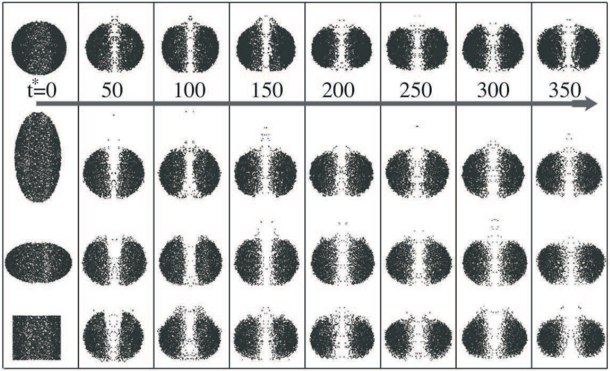

Positions of the point particles integrated over the azimuthal angle

Successive experimental-cloud profiles

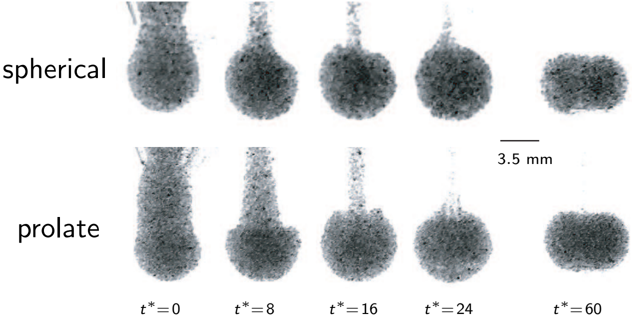

Photographs of the clouds

Evolution of the horizontal-to-vertical aspect ratio γ

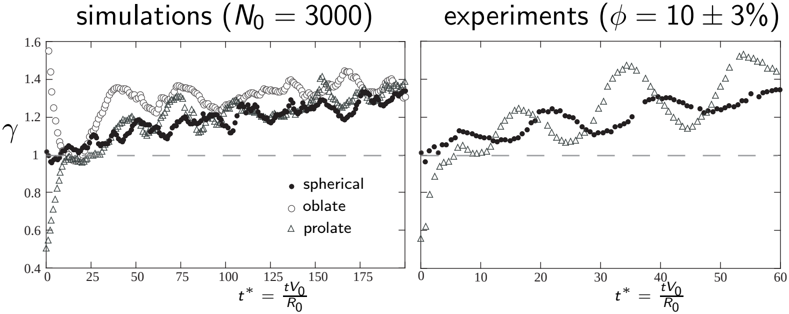

Larger horizontal expansion of the cloud in the experiments

Excluded volume effects not accounted for in the model

Mechanism leading to particle leakage from the cloud

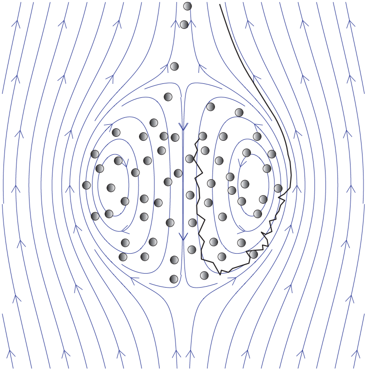

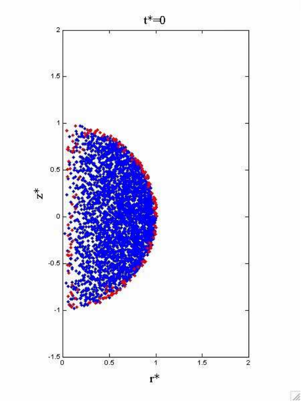

Departure from the closed toroidal circulation due to local unsteadiness of the velocity of the particles

Rate of particle leakage from Nitsche & Batchelor

- Relevant unit of length: mean particle spacing $d = R\left(\frac{4\pi}{3N}\right)^{1/3}$
- Rate-determining factor: velocity of fall of a cloud V
- Rate of particle leakage:

$$-\frac{dN}{dt} \propto \frac{V}{d}$$

- Linear increase in time:

$$\frac{N_0 - N}{N_0^{1/3}} \propto \frac{tV_0}{R_0}$$

for point particle simulations having a small number of particles, $20 \leqslant N_0 \leqslant 320$, over a typical time interval $0 \leqslant t^* = \frac{tV_0}{R_0} \leqslant 120$ (Nitsche & Batchelor JFM 1997)

Experiments versus simulations

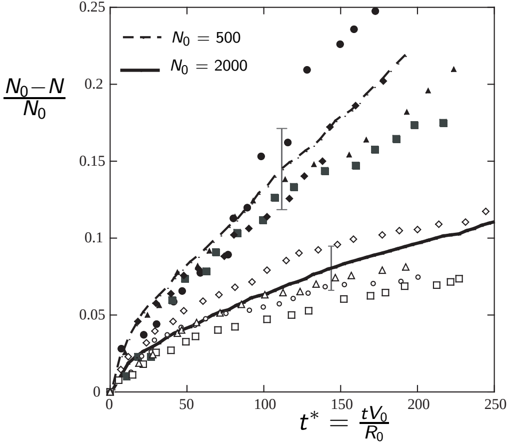

Decrease of the rate of fractional particle leakage with increasing N_0

Numerical scaling

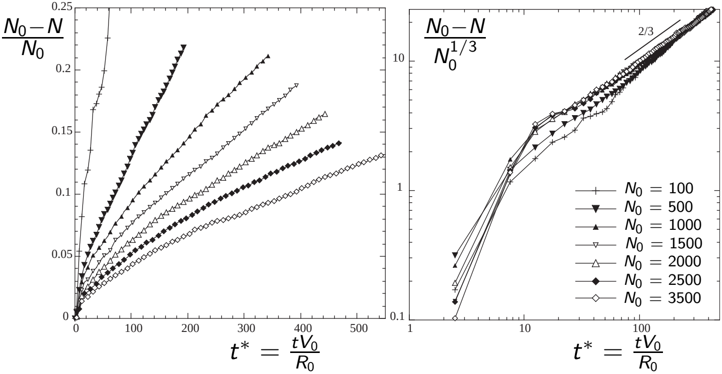

$$\frac{N_0 - N}{N_0^{1/3}} \propto \left(\frac{tV_0}{R_0}\right)^{2/3}$$ for large t^* and N_0

Instability and breakup

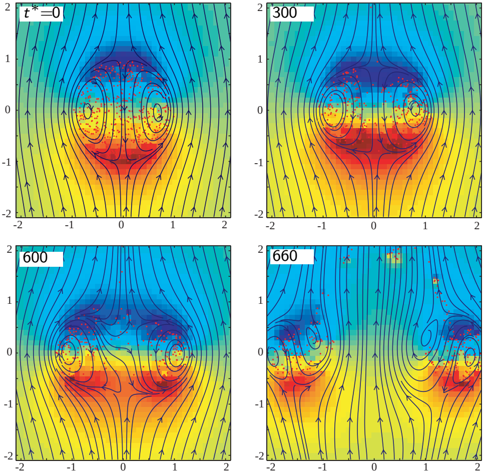

Computed pressure and flow fields

Physical insight using a cloud having a torus shape

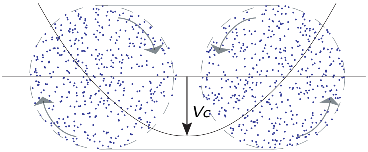

in the cloud reference frame

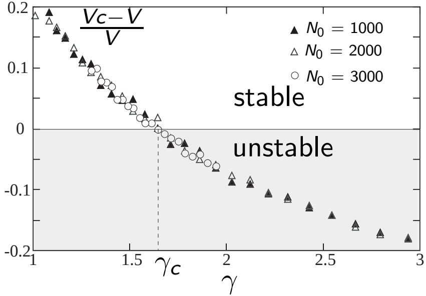

- For $\gamma \geqslant \gamma_c = 1.64 \pm 0.05$, the streamlines pass through the hole in the centre of the torus
- Break-up = change in flow configuration created by the point particles when γ reaches γ_c

Criterion for destabilisation

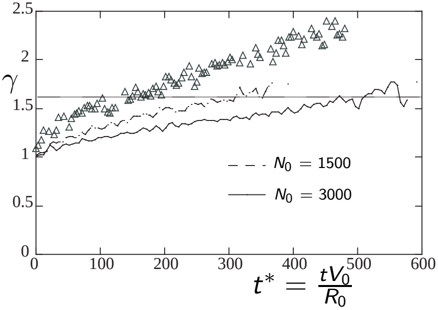

- In point-particle simulations for different $N_0 = 1500$ and 3000, break-up at $\gamma_c \approx 1.64$
- In experiments for $N_0 \approx 1500$ ($\phi = 20 \pm 3\%$), break-up occurs for a larger $\gamma_c \approx 2.4$

Faster evolution!

Experiment Simulation

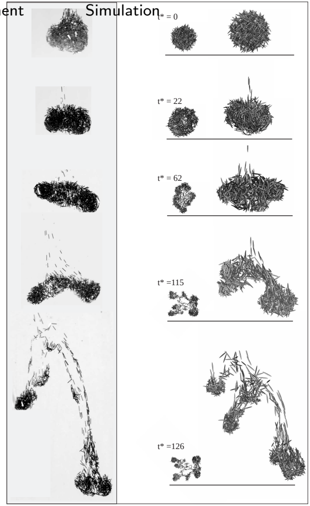

Minimal description: The “fiblet”

- Dimensionless equation for translational velocity

$$\dot{\mathbf{r}}^*_\alpha = \frac{5c}{8N_0}\left(\mathbf{I} + \mathbf{p}_\alpha\mathbf{p}_\alpha\right)\cdot\mathbf{e}_g + \frac{5}{8N_0}\sum_{\beta\neq\alpha}^{N_0}\left(\frac{\mathbf{I}}{|\mathbf{r}^*|} + \frac{\mathbf{r}^*\mathbf{r}^*}{|\mathbf{r}^*|^3}\right)\cdot\mathbf{e}_g$$

  with $c = 2R_0\ln(2A)/l$ and aspect ratio $A = l/d$

- Dimensionless equation for rotational velocity

$$\dot{\mathbf{p}}^*_\alpha = \frac{5}{8N_0}\left(\mathbf{I} - \mathbf{p}_\alpha\mathbf{p}_\alpha\right)\cdot\sum_{\beta\neq\alpha}^{N_0}\left[\frac{(\mathbf{r}^*\cdot\mathbf{p}_\alpha)\,\mathbf{I} - \mathbf{p}_\alpha\mathbf{r}^* - \mathbf{r}^*\mathbf{p}_\alpha}{|\mathbf{r}^*|^3} + \frac{3\,(\mathbf{r}^*\cdot\mathbf{p}_\alpha)\,\mathbf{r}^*\mathbf{r}^*}{|\mathbf{r}^*|^5}\right]\cdot\mathbf{e}_g$$

Self-term prevails over hydrodynamic interactions between the particles as c becomes large relative to N_0

Evolution of the fiblet cloud

Break-up time

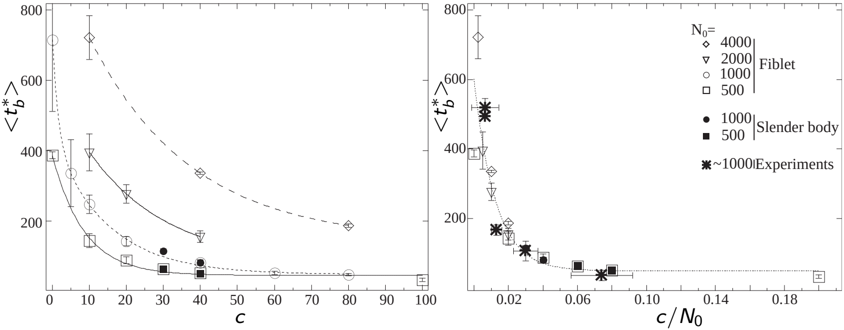

Sole dependance on c/N_0 (self motion of the anisotropic particles)

Park, Metzger, Guazzelli & Butler JFM 2010

Influence of the self-term on the rate of growth

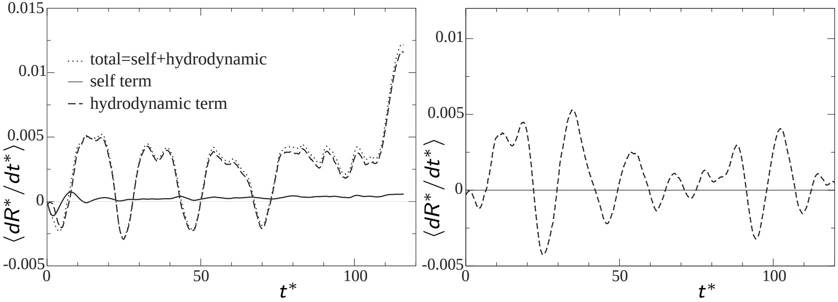

Faster expansion and accelerated breakup for $c = 10$ (left) than for no self term $c = 0$ (right)

Oseen solution

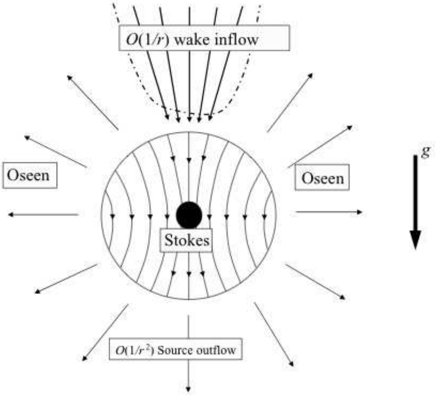

Loss of fore-aft symmetry above inertial screening length

$$\ell = a/Re = \nu/U_0$$

Oseen 1910

Dimensional analysis

- Seven independent physical quantities:
  - Viscosity μ and density ρ_f of the fluid
  - Radius a and density ρ_p of the particles
  - Radius R_0 and number of particles N_0 of the cloud
  - Gravitational acceleration g
- Underlying consideration: long range interactions dominant – short range interactions neglected (no dependance on a/R_0)
- Appropriate dimensionless numbers:
  - N_0 or $\phi = N_0(a/R_0)^3$
  - Dimensionless inertial length $\ell^* = \ell/R_0 = (a/R_0)/Re_p$ or particle Reynolds number $Re_p = U_0 a\rho_f/\mu = (a/R_0)/\ell^*$
  - Cloud Reynolds number $Re_c = V_0 R_0 \rho_f/\mu$
  - Stokes number $St = \frac{2}{9}(\rho_p/\rho_f)Re_p \ll 1$

Regimes of evolution for a sedimenting cloud

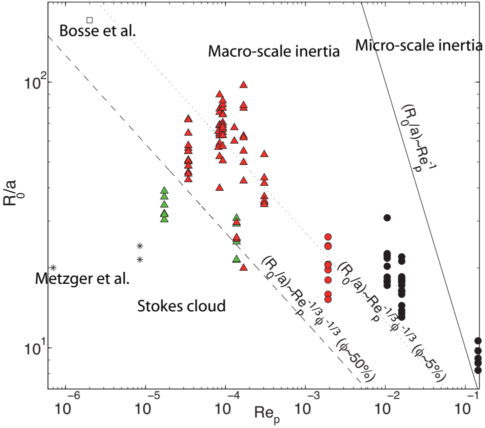

inspired by Subramanian & Koch JFM 2008

Macro-scale inertia

Navier-Stokes equations solved in Fourier space – Lagrangian point-particle tracking – two-way coupling (Bosse, Kleiser, Härtel & Meiburg PoF 2005) + Experiments in 'Macro-scale inertia' regime

Macro-scale inertia: Simulations

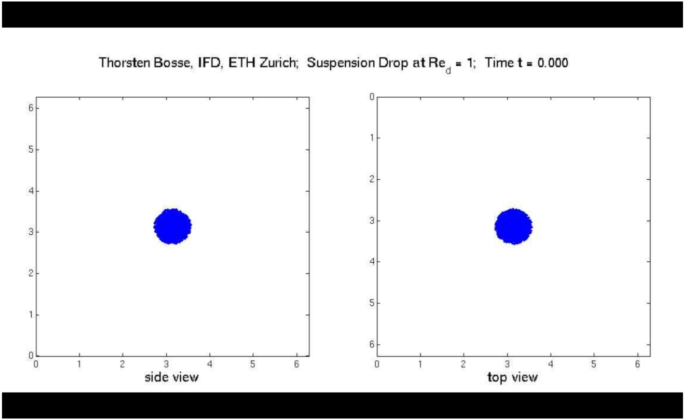

$Re_c = 1$, $N_0 = 100096$, and $\ell^* = 2600$
Bosse, Favre, Meiburg & Kleiser PoF 2005 (Gallery of Fluid Motion, 57th APS/DFD)
Bosse, Kleiser, Härtel & Meiburg PoF 2005

Macro-scale inertia: Experiments

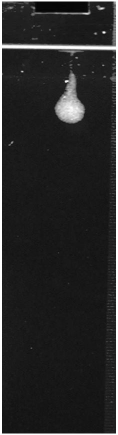

$Re_c = 0.7$, $N_0 = 16000$ and $\ell^* = 179$ ($Re_p = 8 \times 10^{-5}$, $R_0/a = 66$, $\phi = 6\%$, and $St = 2 \times 10^{-5}$)
Pignatel, Nicolas, Guazzelli JFM 2011

Micro-scale inertia

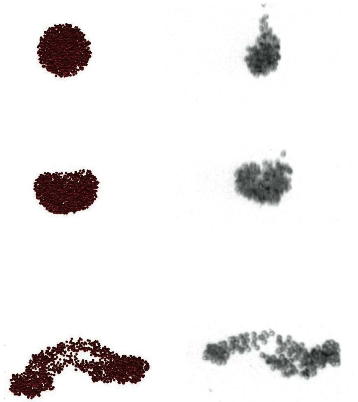

Oseenlet simulations + Experiments in 'Micro-scale inertia' regime

Oseenlet simulations

- Steady Oseen equations still linear (but no longer reversible)

$$\dot{r}_i^\alpha = U_0 \delta_{i3} + \frac{F}{8\pi\mu} \sum_{\alpha \neq \beta} \left\{ \frac{r_i}{r^2} \left[\frac{2\ell}{r}(1-E) - E \right] + \frac{E}{r} \delta_{i3} \right\}$$

with $r_i \equiv r_i^\alpha - r_i^\beta$, $E = \exp(-(1 + x_3/r) r/2\ell)$, gravity $i = 3$

- Dimensionless equations (length-scale $= R_0$ and velocity-scale $= V_0 = \frac{N_0 F}{5\pi\mu R_0}$ of the initially spherical cloud)

$$\dot{r^*}_i^\alpha = \frac{5}{8N_0} \sum_{\alpha \neq \beta} \left\{ \frac{r_i^*}{r^{*2}} \left[\frac{2\ell^*}{r^*}(1-E) - E \right] + \frac{E}{r^*} \delta_{i3} \right\}$$

inspired by Subramanian & Koch JFM 2008

Micro-scale inertia: Simulations

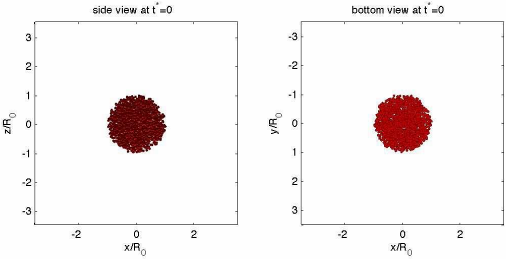

Oseenlet simulations with $N_0 = 2000$ and $\ell^* = 1$

Micro-scale inertia: Experiments

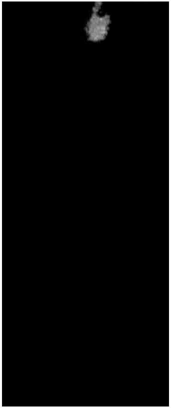

$Re_c = 15$, $N_0 = 600$ and $\ell^* = 0.65$ ($Re_p = 0.14$, $R_0/a = 11$, $\phi \approx 50\%$, and $St = 0.077$)
Pignatel, Nicolas, Guazzelli JFM 2011

Break-up time

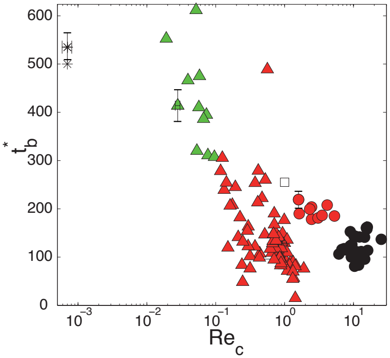

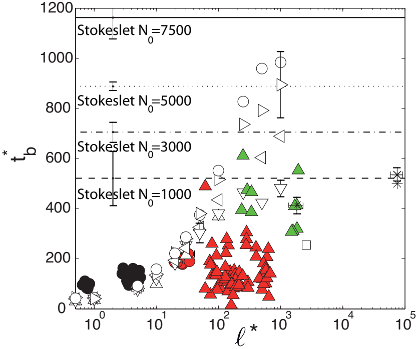

Two clear regimes of macro and micro-inertia!

Mechanisms for torus transition and breakup

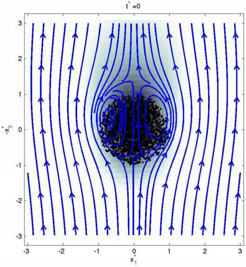

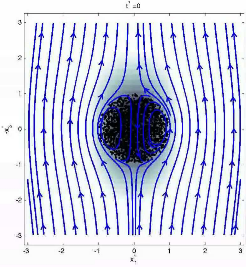

$N_0 = 2000$ and $\ell^* = 1$ (left) and $\ell^* = 20$ (right)

- Evolution toward a torus shape due to fluid inflow instead of particle depletion in Stokes regime
- Breakup at larger aspect ratio than in Stokes regime because front incoming-flow has to overcome the rear incoming-flow

Conclusions

- Multi-body hydrodynamic interactions + coupling between hydrodynamics and the micro-arrangement of the particles → collective dynamics
- While the suspension may be modeled as an effective medium of excess mass, the discrete nature of the suspension is a fundamental ingredient in understanding the observed phenomena
- Different regimes (Stokes, inertia, . . .)
- Success of point-particle approach (even though excluded volume effects not accounted for)

Collaborations

- B. Metzger & F. Pignatel (IUSTI Marseille)
- M. Nicolas (IUSTI Marseille)
- M. L. Ekiel-Jeżewska (IPPT-PAN Warsaw)
- J. E. Butler & J. Park (University of Florida)